GEOLOGY AND GEOPHYSICS

ACTIVE GEODYNAMICS OF THE CAUCASUS REGION: IMPLICATIONS FOR EARTHQUAKE HAZARDS IN AZERBAIJAN

F.A.Kadirov[1], M.Floyd[2], R.Reilinger[2], Ak.A.Alizadeh[1], I.S.Guliyev[1], S.G.Mammadov[1], R.T.Safarov[1]

1 – *Institute of Geology and Geophysics, Azerbaijan National Academy of Sciences, 119, H.Javid ave., Baku, AZ1143*

2 – *Massachusetts Institute of Technology, Cambridge, USA*

In this paper we present GPS observations of crustal deformation in the Africa-Arabia-Eurasia zone of plate interaction, and use these observations to constrain broad-scale tectonic processes within the collision zone of the Arabian and Eurasian plates. Within this plate tectonics context, we examine deformation of the Caucasus system (Lesser and Greater Caucasus and intervening Caucasian Isthmus) and show that most crustal shortening in the collision zone is accommodated by the Greater Caucasus Fold-and-Thrust Belt (GCFTB) along the southern edge of the Greater Caucasus Mountains. The eastern GCFTB appears to bifurcate west of Baku, with one branch following the accurate geometry of the Greater Caucasus, turning towards the south and traversing the Neftchala Peninsula. A second branch (or branches) may extend directly into the Caspian Sea south of Baku, likely connecting to the Central Caspian Seismic Zone (CCSZ). We model deformation in terms of a locked thrust fault that coincides in general with the main surface trace of the GCFTB. We consider two end-member models, each of which tests the likelihood of one or other of the branches being the dominant cause of observed deformation. Our models indicate that strain is actively accumulating on the fault along the ~200 km segment of the fault west of Baku (approximately between longitudes 47-49°E). Parts of this segment of the fault broke in major earthquakes historically (1191, 1859, 1902) suggesting that significant future earthquakes (M~6-7) are likely on the central and western segment of the fault. We observe a similar deformation pattern across the eastern end of the GCFTB along a profile crossing the Kur Depression and Greater Caucasus Mountains in the vicinity of Baku. Along this eastern segment, a branch of the fault changes from a NW-SE striking thrust to an ~ N-S oriented strike-slip fault (or in multiple splays). The similar deformation pattern along the eastern and central GCFTB segments raises the possibility that major earthquakes may also occur in eastern Azerbaijan. However, the eastern segment of the GCFTB has no record of large historic earthquakes, and is characterized by thick, highly saturated and over-pressured sediments within the Kur Depression and adjacent Caspian Basin that may inhibit elastic strain accumulation in favour of fault creep, and/or distributed faulting and folding. Thus, while our analyses suggest that large earthquakes are likely in central and western Azerbaijan, it is still uncertain whether significant earthquakes are also likely along the eastern segment, and on which structure. Ongoing and future focused studies of active deformation promise to shed further light on the tectonics and earthquake hazards in this highly populated and developed part of Azerbaijan.

Introduction and Background

The Geology and Geophysics Institute of the Azerbaijan National Academy of Sciences and the Department of Earth, Atmospheric, and Planetary Sciences at Massachusetts Institute of Technology have been using the Global Positioning System (GPS) to monitor crustal deformation in the territory of Azerbaijan since 1998 (Kadirov et al., 2008). These studies, coordinated and integrated with GPS studies in neighboring parts of the Arabia-Eurasia collision zone, provide new constraints on the fundamental geodynamic processes that are actively deforming the collision zone (e.g. Reilinger et al., 2006; Kadirov et al., 2012; Forte et al., 2012). These geodynamic processes produced and maintain the high elevation of the Turkish-Iranian Plateau (Figure 1) and are the cause of the volcanic and earthquake activity that characterize this region.

The question of earthquake hazards has played a central role in our research because of the increasing vulnerability of the growing population and rapid infrastructure development in Azerbaijan, particularly in the Baku-Absheron region. Azerbaijan has suffered earthquakes historically, including highly destructive earthquakes in 1191, 1859 and 1902 in the Shamakhi region. The 1191 and 1859 earthquakes devastated the then capital city of Shirvan, instigating a relocation of the capital to its present location in Baku (Mushketov, Orlov, 1893; Kondorskaya, Shebalin, 1982). Our GPS studies are part of the Geology and Geophysics Institute's mission that includes understanding the hazards associated with earthquakes: where they are most likely to occur, their expected maximum magnitude, and their likelihood of occurrence. This information is necessary in order to take appropriate preparedness and mitigation measures to reduce the risk to the population and infrastructure, including the vulnerable facilities associated with the petroleum industry that are critical to the economy of Azerbaijan.

In this paper we use GPS observations to constrain Arabia-Eurasia relative plate motions, and the character of inter-plate deformations in the Arabia-Eurasia collision zone. Within this broader context, we focus on earthquake hazards in the Azerbaijan Caucasus and SW Caspian Basin.

Tectonic setting of the Caucasus Mountains

In the broadest context, the Lesser and Greater Caucasus Mountains lie within the zone of plate interaction where the African and Arabian plates are actively converging with the Eurasian Plate (Figure 1). McKenzie et al. (1970), McKenzie (1970, 1972), and Jackson and McKenzie (1984, 1988) provided a plate tectonic description of the region, recognizing active continental collision in eastern Turkey, the Caucasus, and the Zagros; lateral transport of Anatolia (Turkey) towards the west; subduction of African oceanic lithosphere (i.e., Neotethys) along the Hellenic and Cyprus trenches; N-S extension in the Aegean and western Turkey; and ocean rifting along the Red Sea and Gulf of Aden. Convergence of Arabia and Africa with Eurasia has been occurring for > 100 Ma as the intervening Neotethys Ocean lithosphere has been subducting beneath Eurasia. While ocean subduction continues at present along the Hellenic and Cyprus trenches, complete ocean closure north of the Arabian plate occurred ~27 Ma (e.g., McQuarrie, van Hindsbergan, 2013).

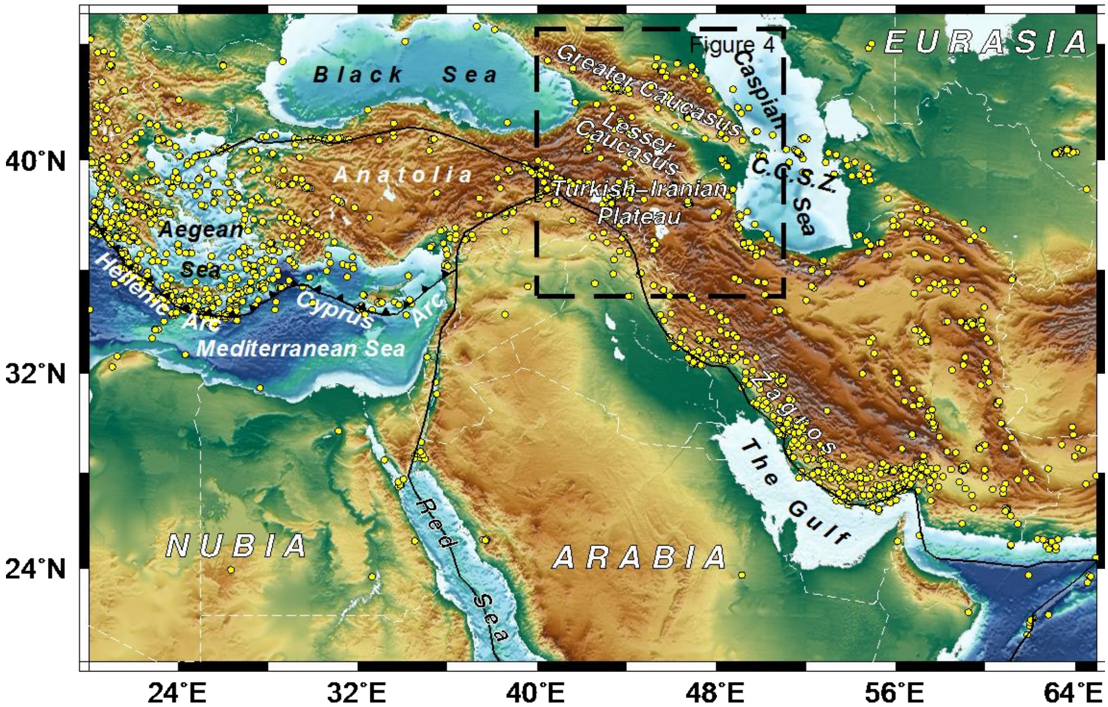

Figure 1. Tectonic overview of the Arabia-Eurasia Collision Zone. Yellow dots are earthquakes from the EHB catalogue (Engdahl et al., 1998) and updates thereof to 2008, plus ISC locations from 2009 onwards. Major plate boundaries are from Bird (2003)

Subsequent seismological, geophysical and geological studies added important refinements to this plate tectonic characterization, including the westward "extrusion" of Anatolia accommodated by the North and East Anatolian faults (Sengor et al., 1985), partitioning of crustal deformation in the eastern Turkey/Caucasus continental collision zone (Jackson, 1992; Allen et al., 2004; Copley and Jackson, 2006), the influence of slab detachment on uplift and volcanism of the Turkish Iranian Plateau (e.g., Sengor et al., 2004; Barazangi et al., 2006), and early subduction of the S Caspian oceanic basin beneath the N Caspian Eurasian continental lithosphere along the central Caspian Seismic Zone (e.g., Jackson et al., 2002).

The Greater Caucasus Mountains are thought to have formed by tectonic inversion of a former back-arc ocean that opened during north-dipping subduction of the Neotethys (e.g. Zonenshain and Le Pichon, 1986; Forte et al., 2012), where the eastern Black Sea, Kur Depression in Azerbaijan and southern Caspian Sea are the remaining remnants of the back-arc basin. Both the timing and spatial evolution of shortening and exhumation remain uncertain with preferred estimates of the timing being Late Miocene to Early Pliocene (e.g. Kopp and Shcherba, 1985; Philip et al., 1989; Vincent et al., 2007). Total shortening across the Greater Caucasus is also uncertain with estimates ranging from 150-400 km (e.g., McQuarrie and van Hindbergen, 2013), and an increase in total shortening from west to east (e.g., Král and Gurbanov, 1996; Avdeev, Niemi, 2008; Forte et al., 2012).

Global Positioning System

During the past ~20 years, the active tectonics of the Africa-Arabia-Eurasia plate system have been measured directly by geodetic observations, most importantly the Global Positioning System (GPS) (Hager et al., 1991; Dixon, 1991). GPS consists of a system of 32 satellites 20000 km above the earth's surface that complete 2 orbits of the earth each 24 hrs (*http://tycho.usno.navy.mil/gpscurr.html).* The satellites are operated by the US Department of Defence in cooperation with the Interagency GPS Executive Board. Other Global Navigation Satellite Systems (GNSS) have been developed by Russia (GLONASS), a European consortium (Galileo), Japan (QZSS), and China (Beidou), but these systems are not used in the results we report.

There are three components to using the GPS system for precise positioning, the satellite constellation, a global network of GPS tracking stations (Mueller, Beutler, 1992), and data processing involving applying physical models and parameter estimation. Most important for this chapter, positions are determined with an accuracy of ~2 mm in horizontal coordinates and 3-10 mm in heights by recording data over a 24-hour period. These precisions are possible because of highly accurate timing provided by atomic clocks on the GPS satellites, precise orbital positions for the satellites provided by the International GNSS Service *(http://igs.org/)* (determined from the global network of observing stations) and processing software that uses advanced mathematical models to account for the Earth's rotation, solid-Earth and ocean tides, and the ionospheric and atmospheric delays of the GPS signal, among other factors that influence position estimates (e.g. Herring et al., 2010).

Estimating surface motions from GPS observations

The GPS measurements presented in this chapter include recording stations (cGPS) that remain in place indefinitely (Figure 2A), and survey-mode (sGPS) observations where the GPS antenna is positioned temporarily over a survey marker (Figure 2B). By repeating these GPS measurements episodically, we are able to estimate how the position has changed during the observation period. cGPS observations allow estimation of position on a daily basis, or more frequently. However, reliable estimates of long-term, secular site velocities require a minimum of 2.5 years of observations even for continuously recording stations because annual and semi-annual systematic errors can bias estimates of steady state motion (Blewitt, Lavellee, 2002).

While the precision of our site velocities varies with observation period, the GPS horizontal velocities we determine using the GAMIT-GLOBK processing software (Herring et al., 2010) have 1-sigma uncertainties in the range of 0.2-0.9 mm/yr, with most sites <0.5 mm/yr. Because deformation rates across the Greater Caucasus Mountains vary from 2-14 mm/yr from northwest to southeast, these precisions allow us to investigate details of the mountain building processes and associated earthquake hazards.

Velocity estimates are determined in a global reference frame; that is, with respect to the global network of tracking stations. The reference frame is determined and maintained (updated) by the International Terrestrial Reference Frame (ITRF) Service (Altamimi et al., 2007) using well-positioned stations, with a long history of well-behaved observations, located around the globe and accounting for motions of the Earth's tectonic plates. We determine site velocities within the ITRF (2008), but we present them in a reference frame fixed to the Eurasian Plate. It is important to bear in mind that the relative motion between measurement sites (i.e., deformation or strain rate) is invariant to changes in reference frame.

Figure 2. A – GPS continuously recording station located in Sheki, Azerbaijan. B – GPS survey site in the Greater Caucasus. The antenna is precisely located above the mark that is cemented into the bedrock

Present-day Arabia-Eurasia continental collision

Figure 3 shows the velocities of GPS sites in the zone of interaction of the African, Arabian, and Eurasian plates (Reilinger et al., 2006 and updates thereof for sites in Azerbaijan). Virtually all major active tectonic processes are well resolved and quantified by the GPS observations, including the northward motion and counter clockwise (CCW) rotation of the Arabian Plate and active opening of the Red Sea (e.g. ArRajehi et al., 2010), crustal shortening of the Zagros fold and thrust zone in Iran (e.g., Djamour et al., 2010), the CCW rotation of the Turkish region accommodated by the North Anatolian Fault (McClusky et al., 2000; Reilinger et al., 2006), northwest motion of the African Plate with respect to Eurasia (McClusky et al., 2003), and the change from NNW motion of Arabia to NNE motion of the Caucasus system (Reilinger et al., 2006; Vernant and Chery, 2006).

Reilinger et al. (2006) used the GPS velocity field to estimate how AR-EU convergence is partitioned between lateral "extrusion" of crustal blocks and crustal shortening. They found that a large majority (~70%) of the convergence is accommodated by lateral transport and ~15% by shortening along the GCFTB, with the remainder being accommodated by other structures or distributed strain. The only slightly thickened crust in the Lesser Caucasus-E Turkey Plateau (Gok et al., 2003; Barazangi et al., 2006), in spite of 150-400 km of continental convergence (McQuarrie, van Hindbergen, 2013), indicates that the geodetic results reflect long-term, tectonic deformation processes in the collision zone (i.e., if not for lateral transport, the crust would be expected to be much thicker). The utility of geodetic studies for constraining long-term geodynamic processes finds further support from comparison between present-day, geodetically derived Arabia-Eurasia convergence rates and longer-term plate convergence rates derived from plate tectonic reconstructions (e.g., McQuarrie et al., 2003) that indicate that these plate motions have been remarkably constant (±10-15%) since the onset of continental collision in the Early Miocene (e.g., ArRajehi et al., 2010).

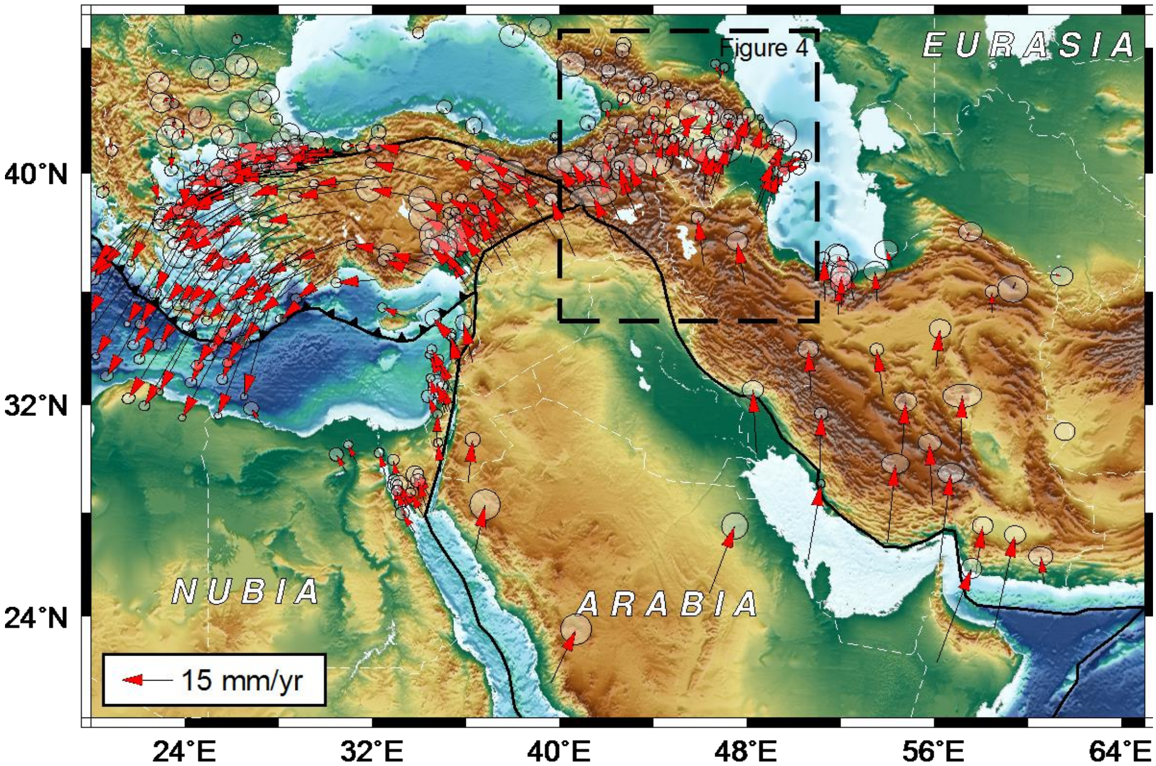

Figure 3. GPS velocities and 95% confidence ellipses with respect to Eurasia (according to Altamimi et al., 2012) within the Eastern Mediterranean from Reilinger et al. (2006), with updated velocities in Azerbaijan for the period 1994.0-2013.5. Major plate boundaries are from Bird (2003), as in Figure 1

Deformation of the Greater and Lesser Caucasus

Figure 4 shows a close-up of the GPS velocity field around the Greater and Lesser Caucasus, providing a quantitative basis to estimate the locations and slip rates and directions on the major structures that accommodate deformation. As is clear from Figure 4, the main shortening in the Arabia-Eurasia collision zone occurs along the southern boundary of the Greater Caucasus near the seismically active Greater Caucasus Fold-and-Thrust Belt (GCFTB). This is well illustrated in the series of velocity profiles in Figure 5, which show the rate of motion versus distance along profiles parallel to (5A) and traversing (5B-E) the Caucasus system (profile locations on Figure 4). Figure 5A shows the component of velocity perpendicular to the direction of the profile**;** Figures 5B-E show the component along the direction of the profile (i.e. shortening or lengthening).The plot in Figure 5A for the profile aligned along strike of the Greater Caucasus demonstrates the progressive increase in convergence rate with Eurasia from west to east, from 1-2 mm/yr near the eastern end of the Black Sea, to 13-14 mm/yr south of Baku, Azerbaijan. The absence of any consistent change in rates in the direction of the profile traversing the Lesser Caucasus (i.e., Figures 5B, 5D and 5E) constrains active shortening in the Lesser Caucasus to < 2 mm/yr. These observations, and the low level of significant seismicity in the Lesser Caucasus (Figure 1; the M6.8, 1988, Spitak, Armenia Earthquake being a notable exception), suggest that, within the resolution of our GPS observations, the Lesser Caucasus behaves like a coherent block rotating in a counter clockwise sense with respect to Eurasia, around a pole near the eastern end of the Black Sea (e.g. Lawrence, 2003; Reilinger et al., 2006; Copley, Jackson, 2006). Rotation may be related to the closure of an inter-continental back-arc basin separating the Lesser and Greater Caucasus with the Caucasian Isthmus (Kur Depression in Azerbaijan) being the last remnants currently undergoing the final stages of subduction/closure (e.g., Cowgill et al., 2012).

Geometry of the eastern GCFTB

The nature of the eastern GCFTB remains an outstanding question in Caucasus tectonics with implications for earthquake hazards in the greater Baku region (Kadirov et al., 2012). Specifically, the physical connection (i.e., faults or zones of deformation) connecting the GCFTB and the Central Caspian Seismic Zone (CCSZ) (Figure 1) remains uncertain. While both structures accommodate convergence with Eurasia, along the CCSZ it is manifest in moderately deep (~40 km) earthquakes with focal mechanisms indicative of deformation within the subducting plate rather than on the plate interface (Jackson et al., 2002), while the GCFTB has broken historically in shallow (~15-20 km) continental thrust events (e.g., Triep et al., 1995). It is possible that this differences due to differences in the nature of the crust and lithosphere (i.e., rheology) at the junction of the GCFTB and CCSZ, continental for the Kur Depression and oceanic (with very thick and consolidated sediments) in the S Caspian Basin (Knapp et al., 2004, Kadirov, Gadirov, 2014). It is also possible, perhaps likely, that the different modes of accommodating shortening at the plate interface reflect different dynamics, subduction in the CCSZ and continental collision along the GCFTB (e.g., Reilinger et al., 2006;Vernant, Chery, 2006; Copley, Jackson, 2006).

New GPS observations on the Absheron and Neftchala peninsulas, and on the southern edge of the Caspian Basin in Iran make it clear that a branch (or multiple branches) of the GCFTB follows the curved topographic break between the Kur Depression and Greater Caucasus/Absheron Peninsula, having a SSE orientation south of Baku (Figures 4 and 6b). Structures accommodating deformation may merge offshore with the thick, folded sediments south of the Absheron Peninsula. This offshore geometry is supported by GPS velocities in the SW corner of the Caspian Basin in Iran (Djamour et al., 2010) that indicate northerly motion with rates similar to those in the adjacent Lesser Caucasus to the west.

On the other hand, the set of velocity vectors from ~ 50 km SW of Baku (SHIK) to the eastern end of the Absheron Peninsula (GURK) indicate shortening at ~6 mm/yr perpendicular to the easternmost Caucasus (Figure 6a). We interpret these GPS observations to imply that crustal shortening accommodated by the GCFTB is partitioned between NE-SW shortening across the Absheron Peninsula and right-lateral, transpressive deformation S of Baku that joins the system of folded sediments in the SW Caspian Basin (Figure 4, 6a and 6b).

Implications for earthquake hazards in Azerbaijan

Earthquake hazard analysis includes estimating the most likely locations, magnitudes, and time of future earthquakes. We emphasize that it is not possible at present to determine these parameters precisely (e.g., Jordon, 2014). However, with auxiliary information from geology (paleoseismology, geomorphology; e.g., Forte et al., 2012), and seismology (instrumental and historic; e.g., Ambraseys, Melville, 1982; Philip et al., 2001; Jackson et al., 2002), it is possible to make estimates of location and, to a lesser extent, magnitude and time of anticipated events.

Our approach involves identifying zones of rapid, spatially systematic changes in site velocities that we observe occur almost exclusively across known faults (e.g., McClusky et al., 2000; Vernant et al., 2014). To the extent that the velocity changes across the faults are due to strain accumulation, the velocity field provides direct evidence for the likely locations of future earthquakes. Some caution is needed since earthquakes are known to occur in areas of very low strain rates, including the 1988 Spitak, Armenia earthquake. While it is difficult to quantify hazards in such cases, we expect very long repeat times for similar earthquakes (e.g., Westaway, 1990), making their occurrence less likely than earthquakes on faults that are rapidly accumulating strain.

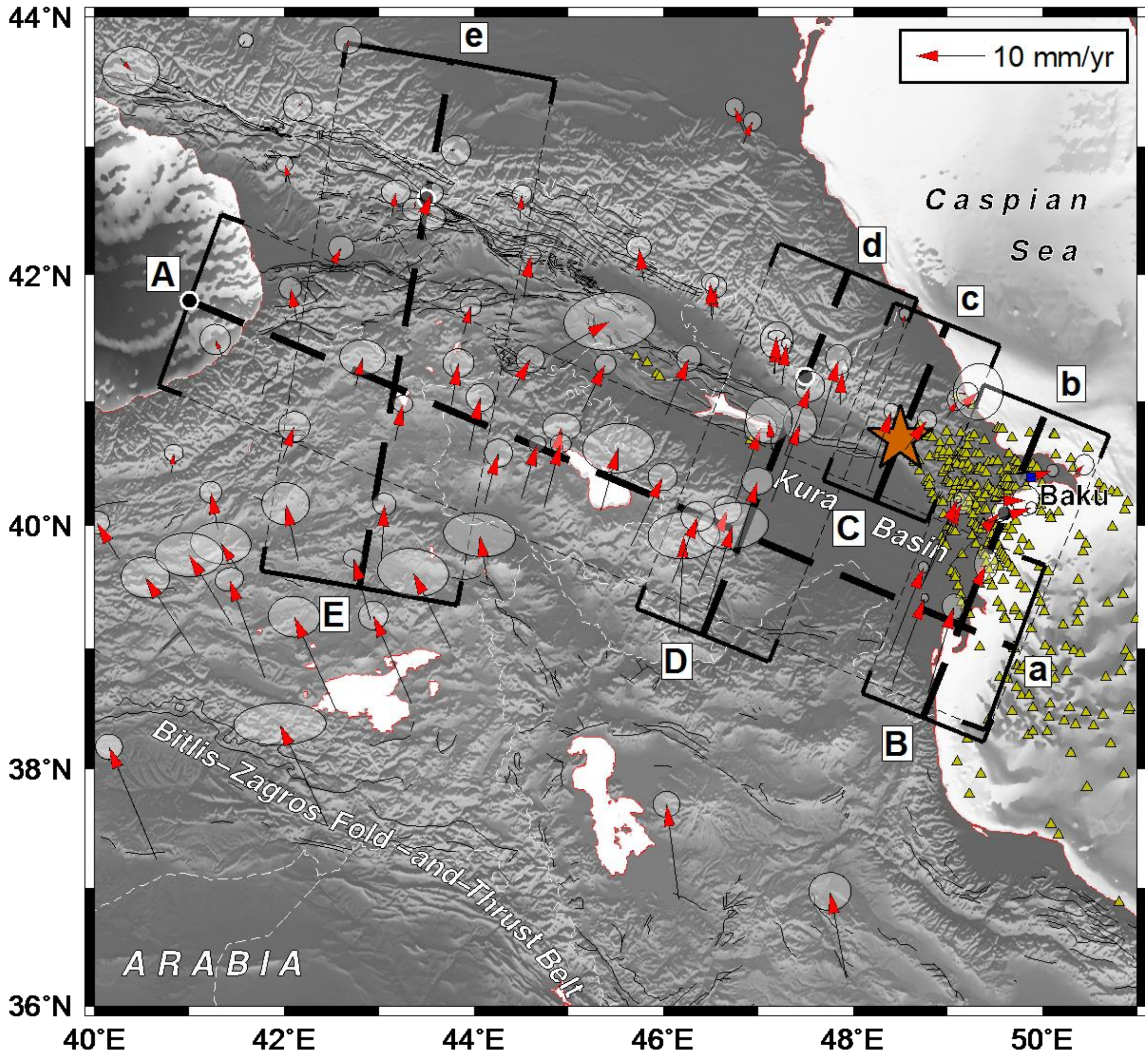

Figure 4. GPS velocities and 95% confidence ellipses w.r.t. (with respect to) Eurasia for the eastern AR-EU collision zone. Orange star shows 1902, M6.9 Shamakha earthquake epicenter. Yellow triangles represent mud volcanoes. Velocity profiles A-E are shown in Figure 5. Their origins are marked by black dots which, for profiles B-E, coincide approximately with the surface expression of the GCFTB

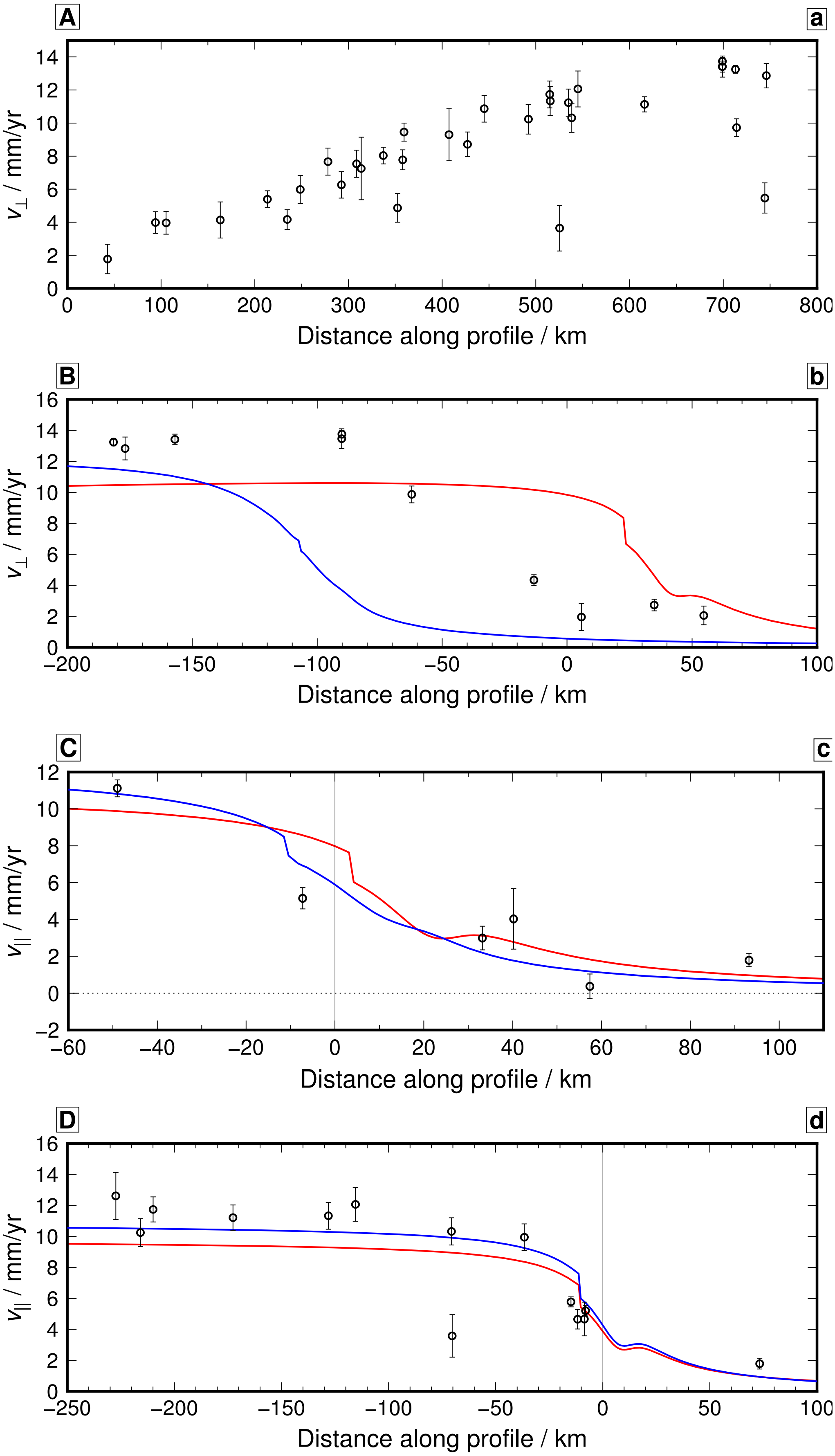
A
a
v⊥ / mm/yr
0 2 4 6 8 10 12 14
0 100 200 300 400 500 600 700 800
Distance along profile / km
B
b
v⊥ / mm/yr
0 2 4 6 8 10 12 14 16
–200 –150 –100 –50 0 50 100
Distance along profile / km
C
c
v|| / mm/yr
–2 0 2 4 6 8 10 12
–60 –40 –20 0 20 40 60 80 100
Distance along profile / km
D
d
v|| / mm/yr
0 2 4 6 8 10 12 14 16
–250 –200 –150 –100 –50 0 50 100
Distance along profile / km

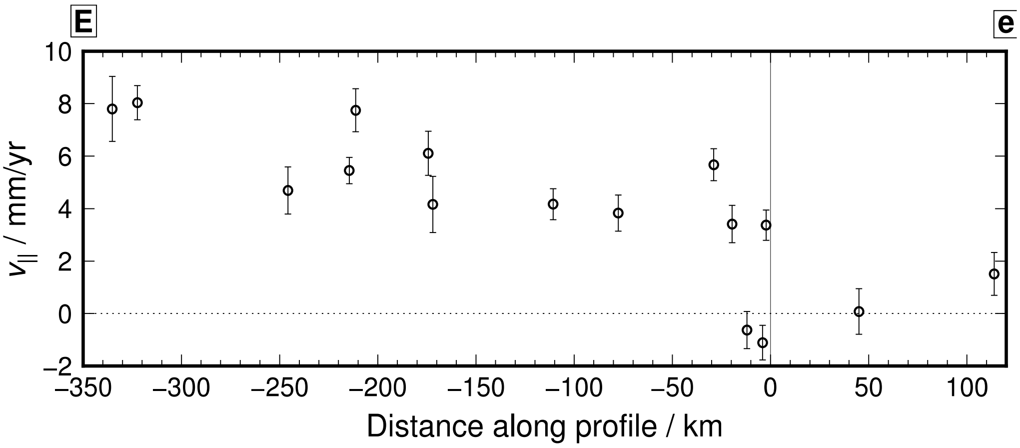

Figure 5. Plots of transverse (A) and parallel (B-E) components of velocities versus distance along the profiles shown in Figure 4. Red curves are velocity profiles from the model shown in Figure 6a, blue curves are velocity profiles from the model shown in Figure 6b (see main text for descriptions). The approximate location of the surface trace of the GCFTB is shown by the vertical line at the origin (see black dots in Figure 4). Note different scales

The magnitude of an earthquake is directly related to the total earthquake offset (co-seismic fault slip) and the surface area of the fault break (Aki, Richards, 2002; Wells, Coppersmith, 1994). Some idea of the possible size of pending earthquakes can be garnered from the historic earthquake record, and/or geological observations of surface faults (e.g., Weldon et al., 2004). With an estimate of the expected magnitude of an anticipated earthquake, we can use the time since the prior event, and the rate of offset accumulation across the fault to estimate the time until the next earthquake (i.e., when the offset accumulation equals the observed co-seismic offset in prior earthquakes).

This simple approach assumes (1) rate differences across the fault are due entirely to strain accumulation for the full time period since the prior earthquake and not permanent deformation or a-seismic slip on the fault (i.e., the fault is fully coupled or locked, and the crust adjacent to the fault is not deforming an elastically); (2) the GPS-determined rate of strain accumulation is constant throughout the period since the prior earthquake; and (3) the fault will fail in an earthquake of similar magnitude to the prior event(s) (i.e., "characteristic earthquake" model; Swartz and Coppersmith, 1984).

Each of these assumptions requires consideration for each individual fault being analyzed (e.g., WGCEP, 2007). Some faults are known to fail aseismically via fault creep up to the surface, either in steady-state or by episodic creep events. Sections of the San Andreas and North Anatolian strike-slip faults are well-studied examples (e.g., Lyons, Sandwell, 2003; Cetin et al., 2014). In fact, below depths of a few 10s of km (i.e., fault locking depths), faults of all types accommodate relative motion aseismically (we exclude discussion of deep earthquakes in the subducting lithosphere). However, we are not aware of evidence for shallow, aseismic slip on continental thrust faults such as those within the GCFTB (e.g., Bird, Kagan, 2004).On the other hand, the easternmost segment of the GCFTB may curve to the south taking on a predominantly strike-slip geometry (Figure 6b). To our knowledge, this segment, located south of Baku, has not experienced strike-slip earthquakes during the instrumental period (Jackson et al., 2002). However, whether this segment is creeping aseismically or accumulating strain without generating seismicity (the case for the southern San Andreas Fault; Bennett et al., 1996; Fialko, 2006) remains conjectural.

GPS observations can help address the nature of fault coupling since the spatial pattern of deformation adjacent to a fault has a characteristic strain pattern for a locked fault (e.g., Okada, 1985), and a step-function offset for a freely slipping fault; directly identifiable "end member" cases. Furthermore, the gradient of the velocity near the fault is directly related to the fault locking depth (i.e., below this depth the fault creeps aseismically). Besides directly identifying locked fault segments (i.e., those capable of generating earthquakes), constraining the locking depth is important for estimating fault area, and thus anticipated earthquake magnitude (e.g., Aki, Richards, 2002).

Because the time between moderate to large earthquakes is long compared to the length of time precise fault monitoring observations have been made (beginning in the 1970s with ground-based observations; e.g. Prescott, Savage, 1976), it isn't possible to directly determine the extent to which the rate and spatial geometry of strain accumulation remains constant through the period between earthquakes. While long-term slip rates estimated from offset features and topography agree well (±10%) with present-day GPS slip rates (e.g. Reilinger et al., 2006), rates of strain accumulation on faults are known to vary between earthquakes. An important, well observed case is the period of rapid surface deformation that occurs following earthquakes (postseismic period) (e.g. Nur, Mavko, 1974). Postseismic deformation is thought to be due in part to slip on the fault below the seismogenic depth (at temperatures and pressures where the crust no longer behaves elastically) as it responds to the instantaneous stress transferred by the earthquake (e.g., Pollitz, 1992). As the lower aseismic part of the fault relaxes the coseismic induced stress, it reloads the shallow, seismic segments. This mechanism can either drive after slip on the fault (in essence adding to the total coseismic slip, i.e. total earthquake slip prior to re-locking) or reload the fault, thereby advancing the fault in time towards the next earthquake. Available evidence indicates that all fault types experience postseismic deformation of some kind that impacts the nature of strain accumulation on the earthquake fault.

For the few earthquakes studied in some detail, the postseismic period of rapid strain accumulation or release is short relative to the time between earthquakes (< 5%) (e.g., Lyzenga et al., 2000; Podgorski et al., 2007; Ergintav et al., 2009) and any increase in strain accumulation is to some extent offset by after slip (i.e. after slip releases strain and stress). Although insufficient case studies are available to determine the degree to which postseismic effects bias estimates of earthquake repeat times quantitatively, for the most part we assume this uncertainty is small compared to uncertainties due to deviations from the characteristic earthquake model.

The assumption that faults fail in "characteristic earthquakes" is the most critical and the most uncertain assumption necessary for any earthquake forecast (WGCEP, 2007). Again we are hampered by the long time between earthquakes compared to the instrumental and historic records. Paleoseismic observations help fill this deficit, but the information on prior earthquakes becomes less precise with age. From the scant constraints we have, it is clear that even for faults that adhere to the characteristic earthquake model in a general way, appearing to behave quasi-periodically as evidenced by long historic records, variations in repeat times are high, introducing large uncertainties in timing and magnitude estimates (e.g., Weldon et al., 2004). In spite of this variability, repeating patterns have been reported when sufficiently long histories are available (e.g., Ambraseys, 2002; Zoller et al., 2007; Meghraoui et al., 2012), and the notion that quasi-steady strain build up (as evidenced by geodetic observations) will "periodically" overcome fault friction and lead to an earthquake is physically appealing.

Because of these outstanding uncertainties, rather than making estimates of future earthquake occurrences, we present general hypotheses that we hope will help focus ongoing studies to constrain better active geodynamic processes, present-day fault behavior (locked vs. creeping), and paleoseismic and historic earthquake studies, all of which are needed to reduce forecast uncertainties. Furthermore, our identification of faults that are potentially accumulating strain in Azerbaijan contributes to the development of earthquake scenarios for estimating seismic ground motion, and focusing earthquake preparations and responses (e.g., Jones et al., 2008).

Deformation and possible strain accumulation along the Main Caucasus thrust fault

In Figures 5B, 5C and5D we compare the results of simple, elastic models of strain accumulation for the wide profiles crossing eastern and west-central Azerbaijan (Figure 4). We consider two models; the surface outcrop of both are shown in Figures 6a and 6b, and model parameters (fault locking depth and dip) are given in the caption for Figure 6. Both models include thrusting along the segment of the GCFTB west of the Absheron Peninsula, where the fault dips northward at 30°. Model A has this same fault geometry extending to the east, south of Baku and connecting with the Central Caspian Seismic Zone. Model B has the modeled fault following the topographic break of the GCFTB west of Baku, turning to the south and extending through the Neftchala Peninsula. In this latter model, the fault dip gradually increases with the change in strike to become vertical along the Neftchala Peninsula. The models show the deformation predicted by a fault that is locked to a certain depth and freely slipping below that depth following the formulation of Okada (1985). Figure 6 shows the residual (observed minus estimated) GPS velocities for each model.

Profile D crosses the GCFTB approximately 70 km WNW of the 1902, M6.9, Shamakha Earthquake epicenter. For perspective, a M6.9 thrust earthquake is expected to have a surface rupture length of ~40-70km (Wells and Coppersmith, 1994). The model results for the profile shown in Figure 5D are almost identical for the 2 models considered; both models involve thrust faulting on a 30°dipping fault that is roughly coincident with the GCFTB in west-central Azerbaijan (Figure 6). The width of the zone of shortening is consistent with a fault locked to a depth of at least12 km (measured vertically from the surface) accumulating offset deficit at a rate of 10-12 mm/yr (i.e., offset deficit is the missing slip on the fault that is expected to be released in an earthquake).

Figure 5C shows the shorter and sparser profile crossing the GCFTB at the location of the 1902 Shamakha Earthquake (Figure 4). The Shamakha region experienced earlier, devastating earthquakes in 1191, and 1859. As mentioned earlier, these events were so severe that they instigated the population to move the Azerbaijan capital from Shirvan to the present location of Baku. The total amplitude (~ 11 mm/yr) and distribution of shortening (~ 70-100 km) along this short profile that crosses a segment of the fault system known to generate M~7 earthquakes, is very similar to that for Profile D. In addition, the overall kinematics and morphology of the GCFTB is generally similar along this segment of the range. However, this is approximately the location at which the major GCFTB begins to bifurcate into several potentially active structures. The relatively sparse GPS data along Profile C makes these end-member structures, as previously described and shown by the red and blue curves, indistinguishable. Nevertheless, these observations suggest that the entire GCFTB in Azerbaijan west of the Shamakha earthquake region is likely to experience earthquakes in the future, possibly similar to the historic events near Shamakha.

Profile B (Figure 5b) crosses the Kur Depression, eastern Greater Caucasus, and Absheron Peninsula near Baku (Figure 4). As described earlier, the new GPS observations presented here reveal that the trend and complexity of the eastern most GCFTB near Baku aid us in placing physical constraints on potentially active structures in an area that remains poorly understood. However, large misfits to both models confirm that there is likely to be deformation accommodated both on structures that continue east into the Central Caspian Sea and others that strike southward towards the Neftchala Peninsula. Figures 5B and 6 show that neither end-member model alone satisfactorily explain the observations. Neither model is significantly better than the other: the weighted root-mean-square (WRMS) residual to the model shown in Figure 6a is 2.04 mm/yr and the WRMS for the model shown in Figure 6b is 1.96 mm/yr, which

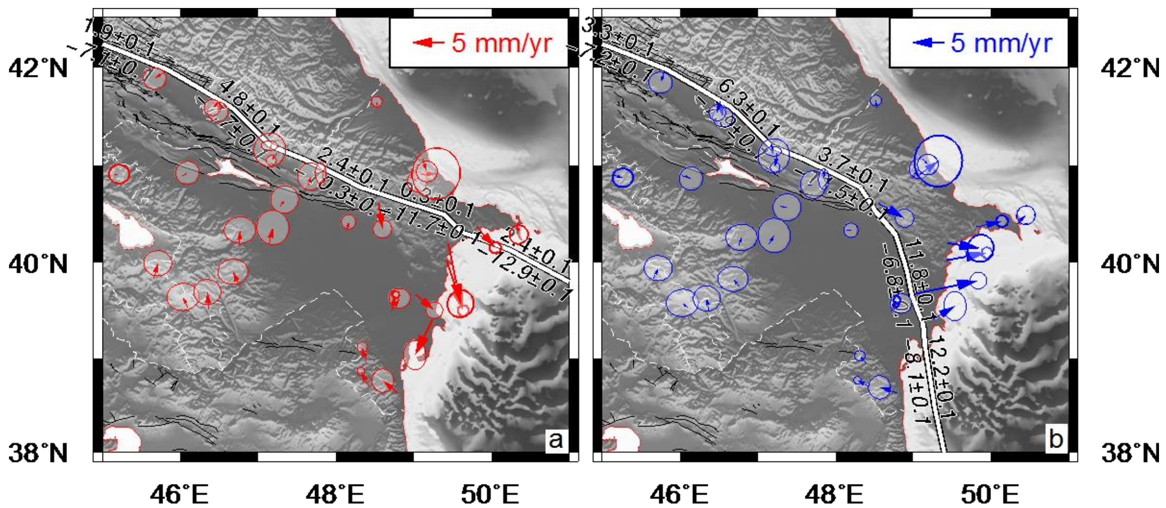

Figure 6. Map showing GPS residual velocities for the two fault models: (a) with continuation of the GCFTB eastwards towards the CCSZ, and (b) with change in strike of the GCFTB southwards along the west coast of the Caspian Sea. The common fault (west of 49.5°E) is a thrust fault dipping north at 30°. In (a), the continuation of the GCTFB is also modeled as a thrust fault dipping north at 30°; in (b) the southward change in strike of the fault is accompanied by a gradual change in dip such that the fault is vertical along the Neftchala Peninsula. All segments of the faults are locked to 12 km depth. Model fault slip rates shown along the fault traces, where the upper number is the strike-slip rate (positive is right-lateral) and the lower number in italics is the dip-slip rate (positive is extension) in mm/yr

is not a statistically significant difference. We do not consider complex models that include multiple branches of the GCFTB here since we have insufficient density of data and lack constraints on motion of the S Caspian Basin southeast of the Absheron Peninsula. We emphasize that these are highly idealized models that do not include variations in elastic properties of the crust, or complexities in the geometry of the eastern GCFTB. More realistic models will require better geodetic constraints on the spatial distribution of motions around the eastern segment.

As indicated in Figures 5 and 6, both these models do provide a good fit to the observed velocities in western Azerbaijan, the Kur Depression, and near Baku and the Absheron region. This gives us confidence about the magnitude of convergent strain rate that must be accommodated by some active structure or structures as we move from western Azerbaijan (convergence at ~ 8 mm/yr) to east (convergence at ~ 12–13 mm/yr). However, significant residual velocities in either one direction or the other exist in the area immediately south-west of the Absheron Peninsula along the coast of the Caspian Sea (Figure 6a compared to Figure 6b) indicating that the exact location and nature of these structures require further investigation. It is likely that a combination of the two modeled faults, possibly along with some other hybrid of intervening structures, is responsible for the observed deformation in this area.

In addition to its arcuate shape and the transition from a shallow dipping thrust fault in the west to a steeply dipping strike-slip fault south of Baku, the easternmost segment of the GCFTB is different in a number of ways from the central thrust segment. For example, the sedimentary section in the southern Caspian Sea south of the Absheron Peninsula reaches thicknesses of > 15 km, roughly twice the thickness of that in the eastern Kur Basin. The Caspian Basin is underlain by ocean crust as opposed to the continental crust below the Lesser Caucasus and Kur depression (e.g., Neprochnov, 1968; Kadinsky-Cade et al., 1981; Jackson et al., 2002). Furthermore, the ubiquitous nature of mud volcanoes in the E Kur Depression (Aliyev et al., 2009) attests to the importance of hydrothermal processes in the crust not present along the GCFTB to the west. How these differences may affect seismogenic structures and earthquake activity is presently unknown.

In spite of these uncertainties, the pattern of deformation across the E branch of the GCFTB (Figure 5B) is very similar to that across the central fault segment (Figures 5C and 5D) that is known to generate significant earthquakes. In addition, the discrepancies between the model fits for our two end-member models (Figures 5B and 6) appear to “bracket” the observations SW of Baku, suggesting that a hybrid-model for strain accumulation is more representative of the actual fault configuration; in this sense, the GPS observations are at least consistent with active strain accumulation. On the other hand, the broad distribution of shortening (Figure 5B) may be due to distributed, aseismic deformation associated with multiple, creeping fault branches, rather than strain accumulation on specific, major faults. Aseismic deformation within the thick, water-saturated sediments of the E Kur Depression seems plausible. We caution however, that the 2011, M9, Fukushima, Japan Earthquake unexpectedly ruptured through the thick, partially consolidated sediments offshore of Japan, producing a substantially larger earthquake than was estimated for the fault, and the accompanying destructive tsunami (e.g., Lay et al., 2011).

Conclusions

Azerbaijan has experienced large (M~7) and highly destructive earthquakes in the past and almost certainly will suffer earthquakes in the future. The geodetic observations presented in this chapter demonstrate that strain is accumulating on the 200 km long segment of the Greater Caucasus Fold-and-Thrust Belt from the Shamakha region (~70 km west of Baku) to the Azerbaijan-Georgian border. Based on the historic earthquake record (destructive earthquakes in 1191, 1859, and 1902) and the geodetic evidence we present for active strain accumulation, M7 thrust earthquakes are likely along this entire segment.

Geodetic observations across the Kur Depression and Absheron Peninsula in the densely populated and highly developed easternmost part of Azerbaijan show a similar deformation pattern across the GCFTB as the observations crossing the central and eastern segments of the fault. While this may indicate active strain accumulation that could generate earthquakes, the absence of large historic earthquakes, the change in strike of the fault west of Baku, and the thick highly saturated sediments in the eastern Kur Depression and south Caspian Basin may preclude large events like those known to occur on the fault further east. However, given the rapid increase in the population and the extensive infrastructural development in this part of Azerbaijan, and the likelihood of gaining new insights from additional geodetic observations and complex fault models, it is essential that further studies be focused on the possibility and effects of damaging earthquakes along the eastern segment of the GCFTB. In particular, densifying GPS coverage along and across the eastern Caucasus, Kur Basin, and Greater Caucasus, constraining the subsurface geometry of the GCFTB and it's extension into the Caspian Sea with seismic studies, and investigating the historic earthquake record and paleoseismic observations to extend the earthquake record will provide the constraints needed to clarify better earthquake hazards in Azerbaijan.

Acknowledgments

We thank UNAVCO for technical support for the GPS network and survey observations. This research was supported by the Azerbaijan National Academy of Sciences, and the US National Science Foundation (NSF grant EAR-1321796).

The research was performed in international laboratory "Modern movements of Earth's crust and geodynamic hazards" at Geology and Geophysics Institute of Azerbaijan National Academy of Sciences within the framework of collaborative research from Massachusetts Institute of Technology (MIT).

REFERENCES

AKI, K., RICHARDS, P.G. 2002. Quantitative seismology. University Science Books. Sausalito, CA. 700 p.

ALLEN, M., JACKSON, J., WALKER, R. 2004. Late Cenozoic reorganization of the Arabia-Eurasia collision and the comparison of short-term and long-term deformation rates. *Tectonics, 23*, TC2008, doi:10.1029/2003TC001530.

ALIYEV, A.A., GULIYEV, I.S., RAHMANOV, R.R. 2009. Catalogue of mud volcanoes eruptions of Azerbaijan (1810-2007). Natfa-Press. Baku.

ALTAMIMI, Z., COLLILIEUX, X., LEGRAND, J., GARAYT, B., BOUCHER, C. 2007. A new release of the international terrestrial reference frame based on time series of station positions and earth orientation parameters. ITRF2005. *J. Geophys. Res*., doi:10.1029/2007JB004949.

AMBRASEYS, N.N. 2002. The Seismic activity of the Marmara Sea region over the last 2000 years. *Seismo. Soc. Am. Bull., 92*, 1-18.

AMBRASEYS, N.N., MELVILLE, C.P. 1982. A history of Persian earthquakes. Cambridge University Press. Cambridge. London, New York, New Rochelle, Melbourne, Sydney. ISBN 0 521 24112 X.

ArRAJEHI, A., McCLUSKY, S., REILINGER, R.E., DAOUD, M., ALCHALBI, A., ERGINTAV, S., GOMEZ, F., SHOLAN, J., BOU-RABEE, F., OGUBAZGHI, G, HAILEAB, B, FISSEHA, S., ASFAW, L., MAHMOUD, S., RAYAN, A., BENDIK, R., KOGAN, L. 2010. Geodetic constraints on present-day motion of the Arabian Plate: Implications for Red Sea and Gulf of Aden rifting. *Tectonics, 29*, TC3011, doi:10.1029/2009TC002482.

AVDEEV, B., NIEMI, N.A. 2008. Constraints on the rates and timing of exhumation of the Greater Caucasus from low-temperature thermochronology. *Eos, Trans. Am. Geophys. Union, 89*, 53.

BARAZANGI, M., SANDVOL, E., SEBER, D. 2006. Structure and tectonic evolution of the Anatolian plateau in eastern Turkey, *Geol. Soc. Am. Special Paper, 409*.

BENNETT, R.A., RODI, W., REILINGER, R. 1996. Global Positioning System constraints on fault slip rates in southern California and northern Baja, Mexico. *J. Geophys. Res., 101*, 21,943-21,960.

BIRD, P. 2003. An updated digital model of plate boundaries. *Geochemistry, Geophysics, Geosystems*, 4(3), 1027, doi: 10.29/2001GC000252.

BIRD, P., KAGAN, Y.Y. 2004. Plate-tectonic analysis of shallow seismicity: Apparent boundary width, beta, corner magnitude, coupled lithosphere thickness, and coupling in seven tectonic settings. *Seismo. Soc. Am. Bull., 94*, 2380-2399.

BLEWITT, G., LAVALLEE, D. 2002. Bias in geodetic site velocity due to annual signals. In: *Vistas for Geodesy in the New Millenium*, Int. Assoc. Geod.Symposia, 125, 499-500.

CETIN, E., CAKIR, Z., MEGHRAOUI, M., ERGINTAV, S., AKOGLU, A.M. 2014. Extent and distribution of aseismic slip on the Ismetpasa segment of the North Anatolian Fault (Turkey) from Persistent Scatterer InSAR. *Geochem. Geophys.Geosyst*., 15, doi:10.1002/ 2014GC005307.

COPLEY, A., JACKSON, J. 2006. Active tectonics of the Turkish-Iranian Plateau. *Tectonics, 25*, TC6006, doi: 10.1029/2005TC001906.

COWGILL, E., NIEMI, N.A., FORTE, A.M., ELASHVILI, M., JAVAKISHVILI, Z., MUMLADZE, T. 2012. Orogen-scale structural architecture and potential seismic sources resulting from Cenozoic closure of a relict Mesozoic ocean basin in the Greater Caucasus. S43J-07, 2012 Spring AGU Meeting.

DIXON, T. 1991. An introduction to the Global Positioning System and some geological applications. *Reviews of Geophys., 29*, 249-276.

DJAMOUR, Y., VERNANT, P., BAYER, R., NANKALI, H.R., RITZ, J.F., HINDERER, J., HATAM, Y., LUCK, B., LEMOIGNE, N., SEDIGHI, M., KHORRAMI, F. 2010. GPS and gravity constraints on continental deformation in the Alborz mountain range, Iran. *Geophys. J. Int., 183*, 1287-1301.

ENGDAHL, E.R., VAN DER HILST. R., BULAND, R. 1998. Global teleseismic earthquake relocation with improved travel times and procedures for depth determination. *Bull. Seismol. Soc. Am., 88*, 722-743,

ERGINTAV, S. et al. 2009. Seven years of postseismic deformation following the 1999, M=7.4, and M=7.2 Izmit-Duzce, Turkey earthquake sequence. *J. Geophys. Res.*, doi: 10.1029/2008JB006021.

FIALKO, Y. 2006. Interseismic strain accumulation and the earthquake potential on the southern San Andreas fault system. *Nature, 441*, 968-971,

FORTE, A., COWGILL, E., BERNARDIN, T., KREYLOS, O., HAMANN, B. 2012. Late Cenozoic deformation of the Kura fold-thrust belt, southern Greater Caucasus. *Geological Society of America Bulletin, 122*, 3-4, 465-486, doi: 10.1130/B26464.1.

GOK, R., SANDVOL, E., TURKELLI, N., SEBER, D., BARAZANGI, M. 2003. Snattenuation in the Anatolian and Iranian plateau and surrounding regions. *Geophys. Res. Lett., 30*, 24, doi: 10.1029/2003GL018020.

HAGER, B.H., KING, R.W., MURRAY, M.H. 1991. Measurements of crustal deformation using the Global

Positioning System. *Ann. Rev. Earth Planet Sci., 19,* 351-382.

HERRING, T.A., KING, R.W., McCLUSKY, S.M. 2010. Introduction to GAMIT/GLOBK Release 10.4. Mass. Inst. of Technology, 48p.

JACKSON, J. 1992. Partitioning of strike-slip and convergent motion between Eurasia and Arabia in eastern Turkey. *J. Geophys. Res., 97*, 12471-12479.

JACKSON, J., McKENZIE, D. 1984. Active tectonics of the Alpine-Himalayan belt between western Turkey and Pakistan. *Geophys. J. R. Astr. Soc., 77*, 185-246,

JACKSON, J., MCKENZIE, D. 1988. The relationship between plate motions and seismic tremors, and the rates of active deformation in the Mediterranean and Middle East. *Geophys. J. R. Astr. Soc., 93*, 45-73.

JACKSON, J., PRIESTLEY, K., ALLEN, M., BERBERIAN, M. 2002. Active tectonics of the south Caspian Basin. *Geophys. J. I, 148*, 214-245.

JONES, L. and 13 others. 2008. The Shake Out Scenario, U.S. Geological Survey Open File Report 2008-1150. California Geological Survey Preliminary Report 25, version 1.0.

JORDAN, T.H. 2014. The prediction problems of earthquake system science. *Seismol. Res. Lett., 85***,** 767-769.

KADINSKY-CADE, K., BARAZANGI, M., OLIVER, J., ISACKS, B. 1981. Lateral variations of high-frequency seismic wave propagation at regional distances across the Turkish and Iranian Plateaus. *Journal of Geophysical Research*, 86: doi: 10.1029/JB080i010p09377. issn: 0148-0227.

KADIROV, F., MAMMADOV, S., REILINGER, R.E., McCLUSKY, S. 2008. Some new data on modern tectonic deformation and active faulting in Azerbaijan (according to Global Positioning System measurements). *Proceedings of the Azerbaijan National Academy of Sciences*, *The Sciences of the Earth, 1*, 82-88.

KADIROV, F., FLOYD, M. ALIZADEH, A., GULIEV, I., REILINGER, R.E., KULELI, S., KING, R., TOKSOZ, M.N. 2012. Kinematics of the eastern Caucasus near Baku, Azerbaijan. *Natural Hazards*, 63, 2, 997-1006; DOI 10.1007/s11069-012-0199-0.

KADIROV, F.A., GADIROV, A.H. 2014. A gravity model of the deep structure of South Caspian Basin along submeridional profile Alborz–Absheron Sill. *Global and Planetary Change, 114*, 66-74, DOI: 10.1016/j.gloplacha.

KNAPP, C.C., KNAPP, J.H., CONNOR, J.A. 2004. Crustal-scale structure of the South Caspian Basin revealed by deep seismic reflection profiling. *Marine and Petroleum Geology 2*, 1073-1081.

KONDORSKAYA, N.V., SHEBALIN, N.V. (Eds.). 1982. New catalogue of strong earthquakes in the USSR from ancient times through 1977. *World Data Centre A for Solid Earth Geophysics*, *Report SE-31*, English translation of Russian original, Boulder, Colorado, USA, 608 pp.

KOPP, M.L., SHCHERBA I.G. 1985. Late Alpine development of the east Caucasus. *Geotectonics*, *19*(6), 497-507.

KRÁL, J., GURBANOV, A.G. 1996.Apatite fission track data from the Greater Caucasus pre-Alpine basement. *Chemieder Erde, 56*, 177-192.

LAWRENCE, S.A. 2003. Kinematically consistent, elastic block model of the Eastern Mediterranean constrained by GPS measurements. M.S. Thesis, Massachusetts Institute of Technology, Cambridge, MA.

LAY, T., YAMAZAKI, Y., AMMON, C.J., CHEUNG, K.F., KANAMORI, H. 2011. The 2011 Mw 9.0 off the Pacific coast of Tohoku Earthquake: Comparison of deep-water tsunami signals with finite-fault rupture model predictions. *Earth Planets Space, 63*, 797-801.

LYONS, S., SANDWELL, D. 2003. Fault creep along the southern San Andreas from interferometric synthetic aperture radar, permanent scatterers, and stacking. *J. Geophys. Res., 108, B1*, 2047, doi:10.1029/2002JB001831.

LYZENGA, G.A., PANERO, W.R., DONNELLAN, A. 2000. Influence of anelastic surface layers on postseismic thrust fault deformation. *J. Geophys. Res., 105*, 3151-3157.

MEGHRAOUI, M., AKSOY, M.E., AKYÜZ, H.S., M. FERRY, DIKBAŞ, A., ALTUNEL, E. 2012. Paleoseismology of the North Anatolian Fault at Güzelkoy (Ganos segment, Turkey): Size and recurrence time of earthquake ruptures west of the Sea of Marmara. *Geochem. Geophys. Geosys., 13*, Q04005, doi:10.1029/2011GC003960.

McCLUSKY, S, .BALASSANIA, A., BARKA, A., DEMIR,C., ERGINTAV, S., GEORGIEV, I., GURKAN, O., HAMBURGER, M., HURST, K., KAHLE, H., KASTENS, K., KEKELIDZE, G. KING, R. KOTZEV, V. LENK, O., MAHMOUD, S. MISHIN, A. NADARIYA, T.M., OUZOUNIS, A., PARADISSSIS, D., PRILEPIN,P., REILINGER, R.E., SANLI, I., SEEGER, H., TEALEB, A., TOKSOZ, M.N., VEIS, G. 2000. GPS constraints on plate kinematics and dynamics in the eastern Mediterranean and Caucasus. *J. Geophys. Res*., *105*, 5695-5719.

McCLUSKY, S., REILINGER, R., MAHMOUD, S., BEN SARI, D., TEALEB, A. 2003. GPS constraints on Africa (Nubia) and Arabia plate motion. *Geophys. J. Int., 155*, 126-138.

McQUARRIE, N., STOCK, J.M., VERDEL, C., WERNICKE, B.P. 2003. Cenozoic evolution of Neotethys and implications for the causes of plate motions. *Geophys. Res. Lett*., 30, doi:10.1029/2003GL017992.

McQUARRIE, N., VAN HINSBERGEN, D.J.J. 2013. Retrodeforming the Arabia-Eurasia collision zone: Age of collision versus magnitude of continental subduction. *Geology, 41*, 315-318.

McKENZIE, D.P. 1970. Plate tectonics of the Mediterranean region. *Nature, 226*, 239-243.

McKENZIE, D.P., DAVIES, D., MOLNAR, P. 1970. Plate tectonics of the Red Sea and East Africa. *Nature, 226*, 243-248.

McKENZIE, D.P. 1972. Active tectonics of the Mediterranean region. *Geophys. J. R. Astron. Soc., 30*, 109-185.

MUELLER, I.I., BEUTLER, G. 1992. The International GPS Service for Geodynamics – Development and Current Structure. *Proceedings of the 6th Symposium on Satellite Positioning*, Ohio State University, Columbus, Ohio.

MUSHKETOV, I.V., ORLOV, A.P. 1893. Catalogue of earthquakes of the Russian Empire. *Notes of Russian Geographic Soc., St.Peterburg, 26*, 582 pp (in Russian).

NEPROCHNOV, Y.U. 1968. Structure of the earth's crust of epicontinental seas: Caspian Black and Mediterranean. *Canad. J. Earth Sci., 5*, 1037-1043.

NUR, A., MAVKO, G. 1974. Postseismic Viscoelastic Rebound. *Science,*183, 204-206.

OKADA, Y. 1985. Surface deformation due to shear and tensile faults in a half-space. *Bull. Seismol. Soc. Am., 75*, 1135-1154.

PHILIP, H., CISTERNAS, A., GVISHIANI, A., GORSHKOV, A. 1989. The Caucasus: An actual example of the initial stages of continental collision. *Tectonophysics, 161*, 1-21, doi: 10.1016/0040-1951(89)90297-7,

PHILIP, H., AVAGYAN, A., KARAKHANIAN, A., RITZ, J.-F., REBAI, S. 2001. Estimating slip rates and recurrence intervals for strong earthquakes along an intracontinental fault: Example of the Pambak-Sevan-Sunik fault (Armenia). *Tectonophysics, 343*, 205-232, doi:10.1016/S0040-1951(01)00258-X.

PODGORSKI, J., HEARN, E., MCCLUSKY, S., REILINGER, R.E., TAYMAZ, T., TAN, O. 2007. Postseismic deformation following the 1991 Racha, Georgia, earthquake. *Geophys. Res. Lett., 34*, L04310, doi:10.1029/2006GL028477.

POLLITZ, F.F. 1992. Postseismic relaxation theory on the spherical earth. *Bull. Seismo.Soc. Am., 82, 1*, 422-453.

PRESCOTT, W.H., SAVAGE, J.C. 1976. Strain accumulation on the San Andreas Fault near Palmdale, California. *J. Geophys. Res., 81*, 4901-4908

REILINGER, R.E., McCLUSKY, S., VERNANT, P., LAWRENCE, S., ERGINTAV, S., CAKMAK, R., OZENER, H., KADIROV, F., GULIEV, I., STEPANYAN, R., NADARIYA, M., HAHUBIA, G., MAHMOUD, S., SAKR, K., ArRAJEHI, A., PARADISSIS, D., AL-AYDRUS, A., PRILEPIN, M., GUSEVA, T., EVREN, E., DMITROTSA, A., FILIKOV, S.V., GOMEZ, F., AL-GHAZZI, R., KARAM, G. 2006. GPS constraints on continental deformation in the Africa-Arabia-Eurasia continental collision zone and implications for the dynamics of plate interactions. *J. Geophys. Res.*, BO5411, doi:10.1029/2005JB 004051.

SENGOR, A.M.C., GORUR, N., SAROGLU, F. 1985. Strike-slip faulting and related basin formation in zones of tectonic escape: Turkey as a case study, in Strike-slip Faulting and Basin Formation. (Biddle, K.T. and N. Christie-Blick, eds.). *Society of Econ. Paleont. Min. Sec. Pub, 37*, 227-264.

SENGOR, A.M.C., TUYSUZ, O., IMREN, C., SAKINC, M., EYIDOGAN, H., GORUR, N., LePICHON, X., RANGIN, C. 2004. The North Anatolian fault: A new look. *Ann. Rev. Earth Planet. Sci., 33*, 1-75.

SWARTZ, D.P., COPPERSMITH, K.J. 1984. Fault behavior and characteristic earthquakes: Examples from the Wasatch and San Andreas Fault Zones. *J. Geophys. Res., 49*, 5681-5698.

TRIEP, E.G., ABERS, G.A., LERNER-LAM, A.L., MISHATKIN, V., ZAKHARCHENKO, N., STAROVOIT, O. 1995. Active thrust front of the Greater Caucasus: The April 29, 1991 Racha earthquake sequence and its tectonic implications. *J. Geophys. Res., 100*, 4011-4033.

VERNANT, P., CHERY, J. 2006. Low fault friction in Iran implies localized deformation for the Arabia–Eurasia collision zone. *Earth and Planetary Sci. Lett.,246*, 197-206.

VERNANT, P., REILINGER, R.E., McCLUSKY, S. 2014. Geodetic evidence for low coupling on the Hellenic subduction plate interface. *Earth, Planet.Sci.,385*, 122-129.

VINCENT, S.J., MORTON, A.C., CARTER, A., GIBBS, S., TEIMURAZ, G.B. 2007. Oligocene uplift of the Western Greater Caucasus: An effect of initial Arabia-Eurasia collision. *Terra Nova. 19*, 160-166, doi:10.1111/j.1365-3121.2007.00731.x.

WELDON II, R. J., SCHARER, K., FUMAL, T., BIASI, G. 2004. Wrightwood and the earthquake cycle: what a long recurrence record tells us about how faults work. *GSA Today, 14(9)*, 4-10.

WELLS, D.L., COPPERSMITH, K.J. 1994. New empirical relationships among magnitude, rupture length, rupture width, rupture area, and surface displacement. *Bull. Seism. Soc. Am., 84*, 974-1002.

WESTAWAY, R. 1990. Seismicity and tectonic deformation rate in Soviet Armenia: Implications for local earthquake hazard and evolution of adjacent regions. *Tectonics*, *9(3)*, 477-503, doi:10.1029/TC009i003p00477.

WORKING GROUP ON CALIFORNIA EARTHQUAKE PROBABILITIES (WGCEP). 2008. The Uniform California Earthquake Rupture Forecast, Version 2 (UCERF 2): U.S. Geological Survey Open-File Report 2007-1437 and California Geological Survey Special Report 203 [http://pubs.usgs.gov/of/2007/1091/].

ZOLLER, G., BEN-ZION, Y., HOLSCHNEIDER, M., HAINZ, S. 2007. Estimating recurrence times and seismic hazard of large earthquakes on an individual fault. *Geophys. J. Int.*, 170, 1300-1310.

ZONENSHAIN, L.P., Le PICHON, X. 1986. Deep basins of the Black Sea and Caspian Sea as remnants of Mesozoic back-arc basins. *Tectonophysics, 123*, 181-211, doi: 10.1016/0040-1951(86)90197-6.